Measurements of The Thermodynamic Properties of HCFC 142b

Naoyuki Yada,* Katsuhiko Kumagai, Takeshi Tamatsu, Haruki Sato, and Koichi Watanabe

Department of Mechanical Engineering, Faculty of Science and Technology, Keio University, 3-14-1, Hiyoshi, Kohoku-ku, Yokohama 223, Japan

This paper reports thermodynamic properties of HCFC 142b, i.e., vapor pressures, the critical pressure, *PVT* properties, and saturated points in a wide range of temperatures from 297 to 443 K, of pressures from 0.3 to 9.4 MPa, and of densities from 71 to 970 kg/m^3, respectively. For HCFC 142b 139 vapor pressure and *PVT* measurements have been accomplished along 17 isochores. The uncertainties of temperature, pressure, and density measurements are less than ±10 mK, ±3.0 kPa, and ±0.1%, respectively. On the basis of the experimental measurements along each isochore, we have determined 7 saturated points (4 saturated liquid and 3 saturated vapor points), and the critical pressure of HCFC 142b. We have also developed a vapor pressure correlation originated from our 69 vapor pressure measurements and compared it with other vapor pressure data and correlations for HCFC 142b. We have also compared our results with saturated liquid density measurements and correlations reported by other investigators.

Introduction

Hydrochlorofluorocarbon 142b (HCFC 142b; CH_3CClF_2, 1-chloro-1,1-difluoroethane) has not been used commercially because of its flammability. It has recently attracted public attention due to its low-ozone-depletion potential. HCFC 142b is suggested as an alternative working fluid for vapor-compression refrigeration systems; particularly, the binary mixture HCFC 22 + HCFC 142b has been suggested as a promising candidate to replace CFC 12 (*1*).

Although HCFC 142b could become a technically important refrigerant, as mentioned above, there are few publications with reliable experimental measurements of its thermodynamic properties. This paper reports 70 *PVT* data along 17 isochores and 69 vapor pressure measurements in a wide range of temperatures from 297 to 443 K, of pressures from 0.3 to 9.4 MPa, and of densities from 71 to 970 kg/m^3. On the basis of these experimental data, we have determined the critical pressure and 7 saturated points for HCFC 142b and developed a vapor pressure correlation.

Experimental Section

The method, apparatus, and procedure of the *PVT* measurements used here have been described in detail in our previous publications (*2*, *3*). The *PVT* measurements of this work were made by the constant volume method coupled with isothermal expansion. Figure 1 shows a schematic diagram of the apparatus used.

The sample density was determined by dividing the mass of HCFC 142b by the inner volume of the sample cell. The inner volume of the sample cell was corrected for changes in temperature and pressure. The sample temperature was measured with a 25-Ω platinum resistance thermometer calibrated on IPTS-68. It was mounted in the vicinity of the sample cell in a thermostated fluid bath. The sample pressure was transmitted through the diaphragm of a differential pressure indicator (DPI) to an external pressure-measuring system by balancing it with the pressure of nitrogen gas, the pressure-transmitting gas. We calibrated the pressure difference of DPI with a Bourdon-tube differential pressure gauge at each temperature before measuring HCFC 142b, because we confirmed that it depends only on temperature. The correction due to mechanical behavior of the DPI is at most 0.1% of the measured sample pressure. The thermodynamic equilibrium of the sample is always maintained by controlling the thermostated bath within ±5 mK and is examined by observing the temperature and pressure always at the same time every quarter hour.

The uncertainty in the calibration of the platinum resistance thermometer is less than ±5 mK, and the bath fluid temperature is controlled within the fluctuation of ±5 mK. Thus the uncertainty of the temperature measurements was less than ±10 mK. Since the total hydrostatic pressure correction is much smaller than 0.5 kPa, it was ignored. The uncertainty of the pressure measurements due to the DPI is less than ±1.0 kPa, that of the air-piston pressure gauge used for the pressure measurements below 4.2 MPa is less than ±0.4 kPa, and that of the oil-piston pressure gauge used in the pressure range above 4.2 MPa is less than ±2.0 kPa. Therefore, the overall uncertainty in the pressure measurements was less than ±1.4 kPa for pressures below 4.2 MPa and less than ±3.0 kPa for those above 4.2 MPa, respectively.

The uncertainty in the density measurements may accumulate after repeated expansions. The uncertainty in mass measurement is less than 0.04%, and that of the inner volume calibration is less than 0.03%. Since no sample in this work was expanded more than three times, the overall uncertainty in the density measurements is estimated not to exceed ±0.1%. The purities of the sample HCFC 142b are 99.985 and 99.853 wt%.

Results

In this work we measured 69 vapor pressures and 70 *PVT* points along 17 isochores. Figure 2 shows the distribution of these data on a *P*–*T* plane. Table I summarizes all the unsmoothed experimental data, in which the asterisk indicates vapor–liquid coexisting data in the two-phase region; i.e., their pressure values are vapor pressures. Since the corresponding density values are calculated by dividing the confined mass by the inner volume of the sample cell, which has been corrected due to experimental temperature and pressure, those indicate the average densities between vapor phase and liquid phase. In Table I, we indicated the temperature on two temperature scales, i.e., IPTS-68 and ITS-90. Temperature on ITS-90 is calculated from that on IPTS-68.

By analyzing these measurements along each isochore, we have determined the saturation points by graphically finding the breaking point of each isochore on the *P*–*T* plane. We determined the saturated liquid point as the breaking point where the slope of the isochore increases, while the saturated vapor point where it decreases. For the isochores near the critical density, however, it is difficult to find the breaking point of each isochore graphically. Hence, we determined saturated points only for seven isochores in the density region above 715 kg/m^3

---

*To whom correspondence should be addressed.

0021-9568/91/1736-0012$02.50/0

Table I. Experimental Data for HCFC 142b[a]

	T,[b] K				T,[b] K				T,[b] K		
ρ, kg/m^3	T68	T90	P, MPa	ρ, kg/m^3	T68	T90	P, MPa	ρ, kg/m^3	T68	T90	P, MPa
71.14*	313.098	313.087	0.5217	404.3*	383.153	383.125	2.5047	713.7	403.208	403.176	3.9729
71.07*	333.131	333.115	0.8749	403.8*	403.175	403.143	3.5767	712.8	423.151	423.116	7.2950
71.00*	353.154	353.133	1.3782	413.2*	323.140	323.127	0.6826	712.4	433.207	433.170	9.0332
70.90	383.163	383.135	1.7356	412.7*	343.156	343.137	1.1037	713.3	413.072	413.038	5.5892
70.83	403.143	403.111	1.8859	412.4*	363.141	363.117	1.6999	719.8*	323.156	323.143	0.6823
71.00*	355.148	355.126	1.4387	412.0*	383.168	383.140	2.5041	719.1*	343.148	343.129	1.1038
70.99*	357.133	357.111	1.4987	411.5*	403.167	403.135	3.5757	718.4*	363.150	363.126	1.6974
70.99	358.133	358.111	1.5254	411.4*	408.117	408.084	3.8961	717.7*	383.156	383.128	2.5048
70.98	359.151	359.128	1.5417	411.3	413.179	413.145	4.2394	717.2*	397.146	397.115	3.2274
70.98	360.147	360.124	1.5513	410.9	433.032	432.995	5.5257	717.1*	398.129	398.098	3.2815
70.93	373.130	373.104	1.6569	410.7	443.179	443.141	6.1944	717.1	399.136	399.105	3.3845
70.87	393.162	393.132	1.8119	411.1	424.508	424.472	4.9703	716.9 *	403.142	403.110	4.0334
70.80	413.177	413.143	1.9618	447.3*	303.337	303.329	0.3945	716.5	413.160	413.126	5.6929
70.76	423.184	423.149	2.0331	446.7*	333.150	333.134	0.8734	716.1	423.170	423.135	7.4078
70.72	433.180	433.143	2.1049	445.4*	393.151	393.121	2.9996	715.6	433.080	433.043	9.1369
70.69	443.158	443.120	2.1759	445.2*	403.160	403.128	3.5748	768.7*	323.141	323.128	0.6821
79.28*	343.114	343.095	1.1035	445.0*	410.168	410.135	4.0357	768.0*	343.131	343.112	1.1043
109.2*	323.117	323.104	0.6819	445.0	410.477	410.444	4.0465	767.2*	363.128	363.104	1.6983
109.1*	343.142	343.123	1.1058	444.7	423.162	423.127	4.9515	766.5*	383.163	383.135	2.5040
109.0*	363.143	363.119	1.6976	444.5	433.185	433.148	5.6724	766.1	393.033	393.003	2.9774
109.0	383.131	383.103	2.3106	444.2	443.175	443.137	6.4010	765.6	403.172	403.140	4.8521
109.0	393.194	393.164	2.4460	449.3*	303.333	303.325	3.9469	764.8	423.195	423.160	8.7901
108.8	403.159	403.127	2.5764	448.9*	323.137	323.124	0.6795	766.2*	391.176	391.146	2.8994
108.7	413.159	413.125	2.7042	446.9*	410.178	410.145	4.0383	766.1*	392.153	392.123	2.9411
108.7	423.196	423.161	2.8300	446.9	410.482	410.449	4.0605	766.0	394.205	394.175	3.1573
108.6	433.183	433.146	2.9523	569.3*	323.179	323.166	0.6827	765.2	413.155	413.121	6.8039
108.5	443.180	443.142	3.0735	568.7*	343.117	343.098	1.1044	803.3*	323.617	323.604	0.6892
108.9*	373.147	373.121	2.0711	568.2*	363.164	363.140	1.6986	802.5*	343.518	343.499	1.1165
108.9	376.157	376.131	2.1915	567.6*	383.139	383.111	2.5012	801.8*	363.129	363.105	1.6983
108.9	377.173	377.146	2.2232	566.4	423.136	423.101	5.3362	892.2*	297.121	297.115	0.3232
108.9	378.166	378.139	2.2393	566.1	433.208	433.171	6.3869	890.3*	343.139	343.120	1.1069
108.9	379.137	379.110	2.2529	565.8	443.230	443.192	7.4510	889.4*	363.139	363.115	1.7008
149.4*	323.147	323.134	0.6906	638.2*	323.191	323.178	0.6826	888.4	383.147	383.119	6.2724
149.2*	343.150	343.131	1.1034	637.9*	333.142	333.126	0.8736	887.8	393.140	393.110	9.3738
183.6*	373.155	373.129	2.0721	637.6*	343.133	343.114	1.1040	889.2*	367.160	367.136	1.8501
183.5*	393.187	393.157	3.0045	637.0*	363.154	363.130	1.6994	889.2*	368.145	368.120	1.8895
183.4	403.171	403.139	3.3620	636.4*	383.142	383.114	2.5034	889.1	369.127	369.102	1.9695
183.2	423.166	423.131	3.8670	635.7*	403.178	403.146	3.5809	888.9	373.051	373.025	3.1720
183.1	433.203	433.166	4.1081	635.3	413.173	413.139	4.6164	970.5*	343.142	343.123	1.1046
183.0	443.152	443.114	4.3324	635.0	423.164	423.129	5.8875	969.6	358.146	358.124	5.6918
183.4	396.175	396.144	3.1650	634.6	433.146	433.109	7.1924	969.2	363.167	363.143	7.7416
183.4	397.177	397.146	3.2006	634.3	443.149	443.111	8.5273	969.0	367.147	367.123	9.3713
183.4	398.159	398.128	3.2272	716.5*	323.108	323.095	0.6818	970.3*	346.140	346.121	1.1834
183.3	413.192	413.158	3.6187	715.8*	343.117	343.098	1.1043	970.3	347.119	347.099	1.2104
405.4*	323.138	323.125	0.6798	715.1*	363.130	363.106	1.6961	970.2	348.125	348.105	1.6049
405.0*	343.059	343.040	1.0742	714.4*	383.156	383.128	2.5012	969.9	353.140	353.119	3.6569
404.7*	363.130	363.106	1.6982								

[a] Values with an asterisk were measured at a state of vapor–liquid coexistence. The values of density fraction in this state are only nominal. [b] T68 = temperature on IPTS-68; T90 = temperature on ITS-90 (calculated from temperature on IPTS-68).

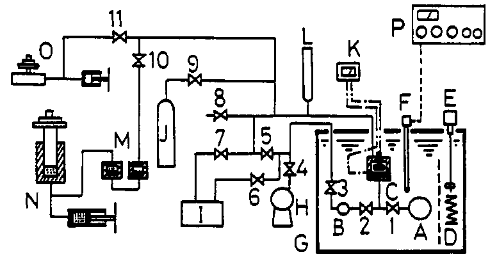

A: Sample cell; B: Expansion cell; C: Differential pressure detector; D: Heater; E: Stirrer; F: Platinum resistance thermometer; G: Thermostated bath; H: Vacuum pump; I: Bourdon tube differential pressure gage; J: Nitrogen cylinder; K: Electronic device for detecting differential pressure; L: Nitrogen gas damper; M: Oil-gas separator; N: Oil-operated dead weight pressure gage; O: Air-piston gage; P: Temperature bridge; 1–11: Valves

Figure 1. Experimental apparatus.

and below 184 kg/m^3. Table II contains four saturated liquid points and three saturated vapor points thus determined. In Table II, the data with an asterisk are saturated vapor points and the others are saturated liquid points.

Discussion

The temperatures under discussion were based on IPTS-68 for convenience in comparing the results of this work with those of other researchers. We determined the critical pressure of HCFC 142b by extrapolating our vapor pressure measurements to the critical temperature determined by Tanikawa et al. (*4*). They determined the critical temperature and density of HCFC 142b by observing the disappearance of the vapor–liquid coexisting meniscus for the same sample used in this work. The determined critical pressure associated with the critical temperature and density determined by Tanikawa et al. (*4*) is as follows:

critical pressure: $P_c = 4.041 \pm 0.002$ MPa

critical temperature (*4*): $T_c = 410.29 \pm 0.02$ K

critical density (*4*): $\rho_c = 446 \pm 5$ kg/m^3

Based upon our vapor pressure measurements and these critical constants, a vapor pressure correlation was developed as follows:

$$\ln (P/P_c) = (-7.0405\tau + 1.1152\tau^{1.5} - 3.5711\tau^{3.5})T_c/T \quad (1)$$

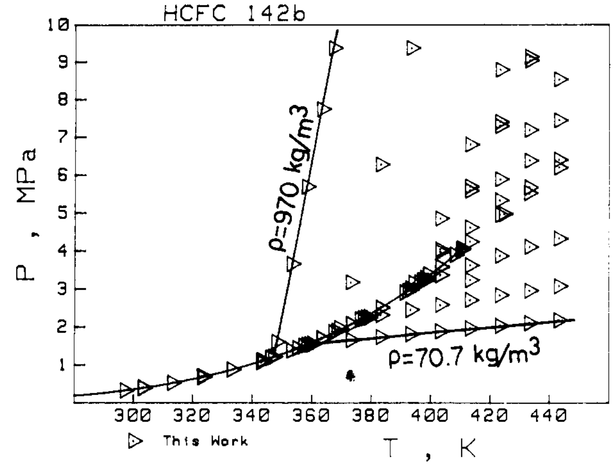

Figure 2. Distribution of experimental data.

Table II. Saturated Points[a]

ρ, kg/m^3	T, K	ρ, kg/m^3	T, K
970	347.0 ± 0.3	183*	396.0 ± 0.5
889	369.0 ± 0.3	109*	375.6 ± 0.8
766	393.2 ± 0.4	71.0*	357.9 ± 0.9
717	398.9 ± 0.5		

[a] Values with an asterisk are saturated vapor points.

where $\tau = 1 - T/T_c$, $T_c = 410.29$ K, and $P_c = 4.041$ MPa.

Equation 1, which is effective for temperatures between 300 K and the critical temperature, reproduces our vapor pressure measurements listed in Table I within ±0.27% of the pressure deviation. Riedel (*5*), Cherneeva (*6*), Valtz et al. (*7*), and Maezawa et al. (*8*) have also reported vapor pressures for HCFC 142b, whereas Riedel (*5*), Mears et al. (*9*), and Cherneeva (*6*) proposed vapor pressure correlations. Although Cherneeva (*6*) has reported thermodynamic properties for HCFC 142, we believe that his results should be for HCFC 142b, since his reported critical constants of HCFC 142 are consistent with those of HCFC 142b reported by others (*5*, *9*). Figure 3 shows the pressure deviations of the present experimental vapor pressures, other available experimental data (*5*-*8*) and reported vapor pressure correlations (*5*, *6*, *9*) from eq 1. It is seen from Figure 3 that the present experimental data and those of Riedel (*5*), Valtz et al. (*7*), and Maezawa et al. (*8*) are in good agreement with the present correlation. The correlation reported by Riedel (*5*) tends to show a large pressure deviation approaching the critical temperature. The behavior of Riedel's correlation arises because Riedel's data do not go above 310 K.

Further, we compared the saturated liquid density listed in Table II with a saturated liquid density correlation reported by Tanikawa et al. (*4*). Figure 4 shows the density deviations of the present saturated liquid density from the correlation by Tanikawa et al., with other saturated liquid density data reported by Riedel (*5*), Cherneeva (*6*), Valtz et al. (*7*), and Maezawa et al. (8). Figure 4 also includes the density deviations of saturated liquid density correlations developed by Riedel (*5*) and Cherneeva (*6*). It is seen from Figure 4 that the present results are in good agreement with the correlation by Tanikawa et al. (*4*) and their experimental data, the data by Valtz et al. (*7*), and Maezawa et al. (*8*), whereas considerable systematic deviations are found from the correlations reported by Riedel (*5*) and Cherneeva (*6*).

As mentioned above, the present results of vapor pressure and saturated liquid density agree well with other reported experimental data and correlations except those of Cherneeva (*6*) and Mears et al. (*9*). The difference between our data and the results reported by Cherneeva (*6*) and Mears et al. (*9*) might be due to the difference in sample purity: Cherneeva (*6*) reported the sample purity of HCFC 142 was 97%, while Mears et al. (*9*) did not mention it.

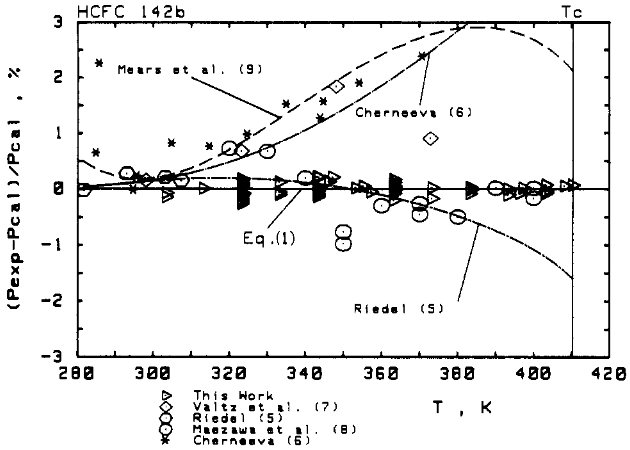

Figure 3. Comparison of vapor pressure data and correlations with eq 1.

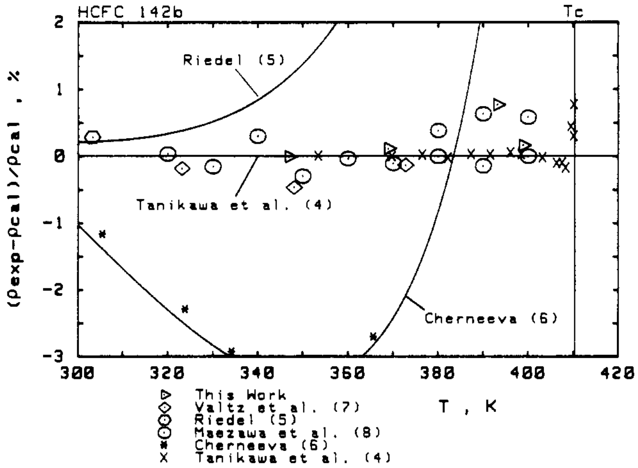

Figure 4. Comparison of saturated liquid density data and correlations with the correlation reported by Tanikawa et al. (*4*).

Acknowledgment

We are greatly indebted to the National Research Laboratory of Metrology, Tsukuba, Japan, for the calibration of the thermometer, to Shin-etsu Chemicals Co., Ltd., Tokyo, for furnishing the silicone oil, to Daikin Industries Co., Ltd., Osaka, and to Asahi Glass Co., Ltd., Tokyo, for kindly furnishing the very pure samples. We also acknowledge Takuhei Simokawa and Mitsuhiro Yudo for their valuable cooperation.

Literature Cited

(1) Yada, N.; Kumagai, K.; Watanabe, K. Proceedings of the 2nd Asian Thermophysical Properties Conference, 1983; p 369.
(2) Takaishi, Y.; Uematsu, M.; Watanabe, K. *Proc. Int. Congs. Refrig.*, *15th* **1978**, *2*, 117.
(3) Takaishi, Y.; Uematsu, M.; Watanabe, K. *Bull. JSME* **1982**, *25* (204), 944.
(4) Tanikawa, S.; Sato, H.; Watanabe, K. *Proc. 30th High Pressure Conf. Jpn.* **1989**, 352.
(5) Riedel, V. L. *Z. Gesamte Kaelte-Ind.* **1941**, *48* (7), 105.
(6) Cherneeva, L. I. *Therm. Eng.* (*Engl. Transl.*) **1958**, *5* (7), 38.
(7) Valtz, A.; Laugier, S.; Richon, D. *Int. J. Refrig.* **1986**, *9*, 282.
(8) Maezawa, Y.; Sato, H.; Watanabe, K. *J. Chem. Eng. Data*, submitted for publication.
(9) Mears, W. H.; Stahl, R. F.; Orfeo, S. R.; Shair, R. C.; Kells, L. F.; Thompson, W.; McCann, H. *Ind. Eng. Chem.* **1955**, *47* (7), 1449.

Received for review February 12, 1990. Accepted July 30, 1990. We are indebted to the grant from Tokyo Electric Power Co., Ltd., Tokyo. We are indebted to the Grant-in-Aid for Scientific Research Fund in 1989 (Project No. 01603022 and 01790369) from the Ministry of Education, Science and Culture, Japan.